Human Molecular Genetics, 2009, Vol. 18, No. 3 ***569–579***
doi:10.1093/hmg/ddn363
Advance Access published on November 3, 2008

A loss-of-function variant of *PTPN22* is associated with reduced risk of systemic lupus erythematosus

Valeria Orrú[1,†], Sophia J. Tsai[2,†], Blanca Rueda[3,†], Edoardo Fiorillo[1], Stephanie M. Stanford[1], Jhimli Dasgupta[2], Jaana Hartiala[1,4], Lei Zhao[1], Norberto Ortego-Centeno[5], Sandra D'Alfonso[6] and The Italian Collaborative Group, Frank C. Arnett[7], Hui Wu[8], Miguel A. Gonzalez-Gay[9], Betty P. Tsao[8], Bernardo Pons-Estel[10], Marta E. Alarcon-Riquelme[11], Yantao He[12], Zhong-Yin Zhang[12], Hooman Allayee[1,4], Xiaojiang S. Chen[2], Javier Martin[3] and Nunzio Bottini[1,*]

[1]Institute for Genetic Medicine, Keck School of Medicine, [2]Molecular and Computational Biology and University of Southern California, Los Angeles, CA, USA, [3]Instituto de Parasitologia y Biomedicina 'Lopez-Neyra', CSIC, Granada, Spain, [4]Department of Preventive Medicine, Keck School of Medicine, University of Southern California, Los Angeles, CA 9033, [5]Department of Internal Medicine, Hospital Clinico San Cecilio, Granada, Spain, [6]Department of Medical Sciences and Interdisciplinary Research Center of Autoimmune Diseases (IRCAD), University of Eastern Piedmont, Novara, Italy, [7]Department of Rheumatology, University of Texas Medical School, Houston, TX, USA, [8]David Geffen School of Medicine, University of California, Los Angeles, CA, USA, [9]Rheumatology Unit, Hospital Xeral-Calde, Lugo, Spain, [10]Sanatorio Parque, Rosario, Argentina, [11]Department of Genetics and Pathology, Rudbeck Laboratory, Uppsala University, Uppsala, Sweden and [12]Department of Biochemistry and Molecular Biology, Indiana University School of Medicine, Indianapolis, IN, USA

Received June 5, 2008; Revised and Accepted October 30, 2008

A gain-of-function R620W polymorphism in the *PTPN22* gene, encoding the lymphoid tyrosine phosphatase LYP, has recently emerged as an important risk factor for human autoimmunity. Here we report that another missense substitution (R263Q) within the catalytic domain of LYP leads to reduced phosphatase activity. High-resolution structural analysis revealed the molecular basis for this loss of function. Furthermore, the Q263 variant conferred protection against human systemic lupus erythematosus, reinforcing the proposal that inhibition of LYP activity could be beneficial in human autoimmunity.

INTRODUCTION

PTPN22 encodes the protein tyrosine phosphatase (PTP) LYP, which is a critical gatekeeper of T-cell receptor (TCR) signaling. In T-cells, LYP (lymphoid tyrosine phosphatase) potently inhibits signaling through dephosphorylation of several substrates, including the Src-family kinases Lck and Fyn, as well as ZAP-70 and TCRzeta (1,2). Recently, *PTPN22* has emerged as an important genetic risk factor for human autoimmunity. Specifically, an R620W missense single nucleotide polymorphism (SNP) (rs2476601) in exon 14 of *PTPN22* is associated with type 1 diabetes (T1D) (3), rheumatoid arthritis (4), systemic lupus erythematosus (SLE) (5), and other autoimmune diseases (reviewed in 6). The R620W substitution occurs within a protein–protein interaction domain and results in a gain of function that inhibits TCR signaling (7,8). Reduced TCR signaling has recently been recognized as a risk factor for autoimmunity and affects disease predisposition by multiple mechanisms, including altered thymic selection, reduced T-helper activity, and decreased number/function of regulatory T-cells (9).

In this study, we sought to determine whether another amino acid substitution, R263Q (G788A, rs33996649) within the catalytic domain of the enzyme, is functional with respect to TCR signaling and phosphatase activity.

*To whom correspondence should be addressed at: USC Institute for Genetic Medicine, 2250 Alcazar Street, CSC 204, Los Angeles, CA 90033, USA. Tel: +1 3234422634; Fax: +1 3234422764; Email: nunzio@usc.edu
†The authors wish it to be known that, in their opinion, the first three authors should be regarded as joint First Authors.

RESULTS

We first compared the effect of the R263Q variant on TCR-induced phosphorylation of intracellular proteins at the single cell level by phospho-specific flow cytometry (Fig. 1A–C). Compared with the wild-type R263 allele (continuous graphs), the Q263 allele (dotted graphs) was less efficient in reducing the phosphorylation of SLP-76, an early mediator of TCR signaling downstream of LYP (Fig. 1C). The Q263 variant was also less efficient in inhibiting the TCR-induced activation of extracellular-signal regulated kinase (ERK) (Fig. 1D) and the TCR-induced activation of an NFAT/AP1 luciferase reporter (Fig. 1E). Taken together, these data suggest that Q263 is a loss-of-function variant of LYP.

Because the R263Q polymorphism is located within the catalytic domain of the phosphatase, we hypothesized that the apparent loss of function is due to reduced phosphatase activity. Consistent with this notion, the phosphatase activity of the Q263 variant was lower than that of R263 (Fig. 2A). To assess this, we generated constructs encoding the catalytic domain of LYP, purified the two allelic variants (Cat-R263 and Cat-Q263, see Fig. 2B), and assayed their activity on a 14-amino acid peptide derived from the Y394 phosphorylation site of Lck, a physiological substrate of LYP. The Cat-Q263 variant showed lower specific activity than Cat-R263 on the physiological peptide (Fig. 2C). Cat-Q263 also showed lower activity than Cat-R263 when two non-specific PTP substrates were used (Fig. 2D and E). Based on these data, we conclude that the R263Q substitution decreases LYP phosphatase activity.

To determine the structural basis underlying this loss-of-function phenotype, we solved the crystal structures of the catalytic domain of the Q263 LYP mutant and the wild-type allele. Based on our new derivation (Fig. 3A; Table 1) as well as that recently reported by Yu *et al*. (10), the overall structure of Cat-Q263 is similar to that of the wild-type allele. However, the $\alpha2'$ helix of Cat-Q263 is significantly displaced (Fig. 3A) as a result of a loss of the stabilizing contact that normally occurs between R263 of $\alpha5$ and Q34 of $\alpha2'$ (Fig. 3B). Thus, substitution of Q at position 263 disrupts the conformation of the loop between the $\alpha1$ and $\alpha2'$ helices, which has been shown to be LYP-specific and to participate in substrate binding (10). This results in an extended $\alpha2'$ helix that exposes the critical S35 residue toward the outer surface of the enzyme. In addition, the flexible Trp-P20-Glu (WPD) loop that provides the hydrophobic pocket, which buries the phosphotyrosine and stabilizes the phosphoryl-cysteine intermediate, is in an open conformation with Cat-Q263, whereas it is half-closed in wild-type LYP (Fig. 3C). Furthermore, a comparison of surface electrostatics between Cat-R263 and Cat-Q263 (Fig. 3D and E) demonstrates that, despite preserving the electropositive nature of the substrate-binding cleft with a hydrophobic boundary, the conformation and depth of the cleft in the Cat-Q263 mutant is different from that of Cat-R263, which could potentially disrupt catalysis. These data provide a plausible molecular mechanism through which the Q263 variant leads to a loss of function. Recently, Yu *et al*. (10) identified a specific small molecule inhibitor of LYP called IC-11. Co-crystallization analysis showed that IC-11 extensively interacts with the same $\alpha1-\alpha2'$ loop, which is affected by the R263Q polymorphism (10). Therefore, we also assessed the inhibitory action of IC-11 on Cat-R263 and Cat-Q263, and found that IC-11 is significantly less potent on the Q263 variant of the phosphatase (Fig. 4), which lends further support to our model of the structural effect of the R263Q polymorphism.

Given that the R620W variant with a gain-of-function effect predisposes individuals to autoimmunity, we reasoned that the loss-of-function nature of the R263Q polymorphism may have a protective effect against autoimmunity. We therefore examined the impact of the R263Q variant on patients with SLE, a systemic autoimmune disease. We genotyped a cohort of 881 SLE patients and 1133 healthy Controls of Caucasian ancestry (Spain) and observed a significant protective effect of the Q263 allele which was present at a higher frequency in Controls compared with Cases [odds ratios (OR) 0.58, 95% confidence interval (CI) 0.38–0.86, $P = 0.006$] (Table 2). To confirm this association, we genotyped the R263Q genetic variant in three independent replication populations (Italian, Argentinean and Caucasian North American). Genotype frequencies were in Hardy–Weinberg equilibrium in patients and Controls in all four populations. The Q263 protective effect was observed in all three cohorts, although the *P*-values did not reach significance likely due to their smaller sample sizes. The Breslow–Day test showed homogeneity of the four populations allowing us to perform a combined analysis with a total of 2093 SLE patients and 2348 Controls, which confirmed the protective effect of the Q263 loss-of-function allele (pooled OR 0.63, 95% CI 0.47–0.84, $P = 0.0017$) (Table 2). It should be noted that these results are obtained from Caucasians and we cannot exclude the possibility that underlying genetic substructure within European-derived populations may affect the association of the R263Q with SLE. This may be particularly relevant in the US cohort, which is a combination of Cases and Controls from two recruitment sites. Previous studies demonstrated that the R620W and the R263Q non-synonymous polymorphisms are in independent *PTPN22* haplotypes (11,12). Therefore, it could be suggested that these genetic variants exert independent effects on genetic susceptibility to SLE. To test this hypothesis, we first examined linkage disequilibrium (LD) between the R620W and R263Q polymorphisms and observed that these variants were completely independent ($r^2 = 0$). Although the low frequency of the R263Q variant precluded a complete test of interaction between the two SNPs, we performed an analysis with the R263Q SNP by conditioning on R620W and observed that the association of the R263Q polymorphism with SLE is independent of the R620W SNP ($P = 0.003$ for the association of R263Q polymorphism conditioned on R620W).

Because the R620W SNP, which predisposes to a variety of autoimmune-related disorders, shows extreme frequency variations among ethnic groups, we sought to determine whether the R263Q SNP also shows population-specific frequency variations. In addition to the four SLE cohorts described earlier, we also genotyped the SNP in African-American, Caucasian, Asian, and Hispanic Control individuals and observed that the frequency of Q263 carriers is $\sim$4% in Caucasians and Hispanics, while carriers are even rarer among African-Americans and Asians (Table 3). Thus, the R263Q SNP does not appear to have significant allele

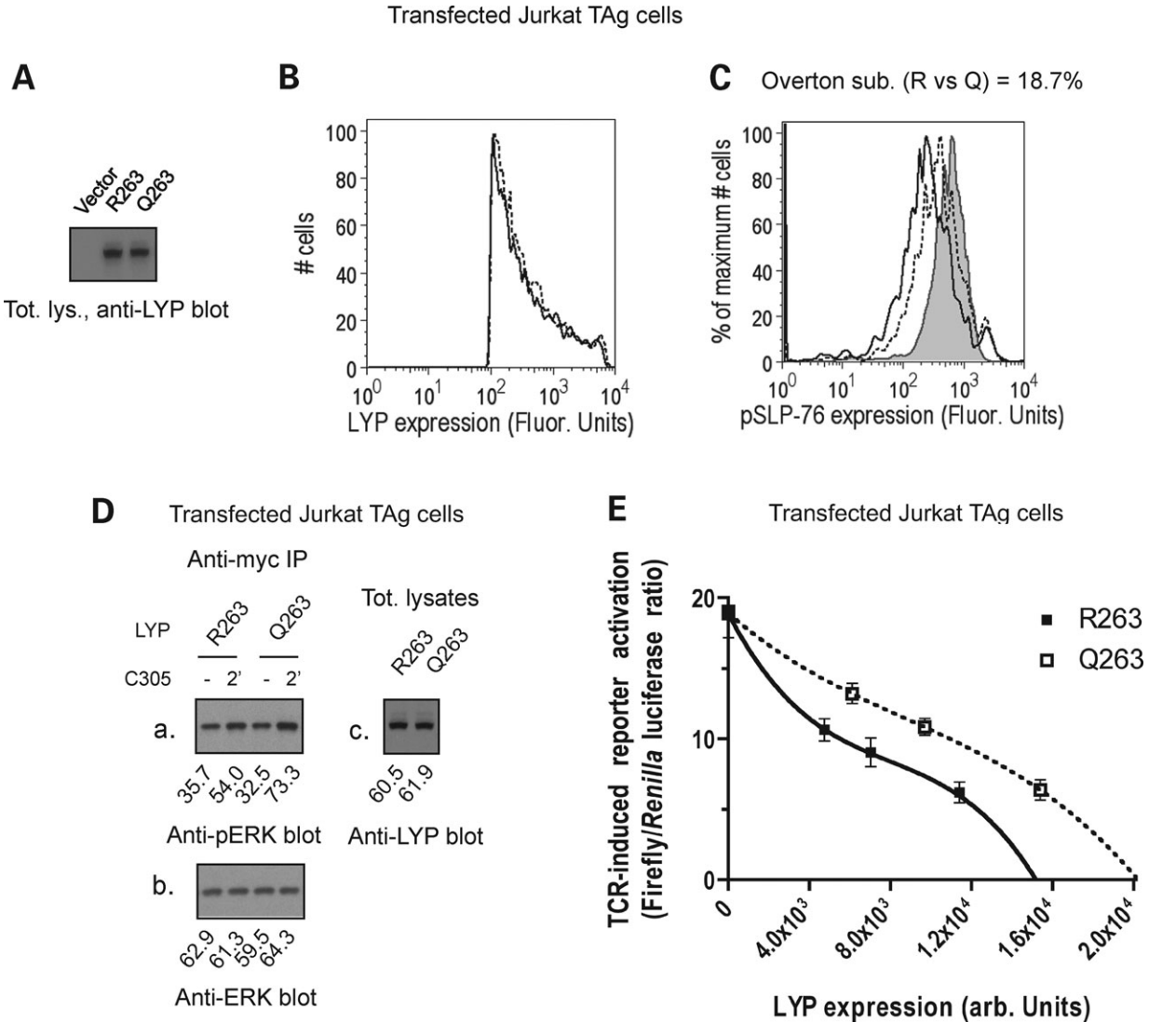

Figure 1. LYP−Q263 is a loss-of-function variant of LYP. (**A**–**D**) Study of the inhibitory activity of LYP−R263 and −Q263 on TCR signaling at the single-cell level. JTAg cells were transfected with LYP−R263 or −Q263 and left unstimulated or stimulated with C305 for 2′. Cells were immediately fixed, permeabilized, and co-stained with an Alexa Fluor488 (AF488)-conjugated anti-LYP antibody and a PE-conjugated anti-pSLP-76(Tyr128) antibody. Cells overexpressing LYP were gated by comparing AF488 fluorescence histograms of transfected and untransfected cells. (A) Anti-HA western blots of total lysates of untransfected cells (lane 1), and cells transfected with HA−LYP−R263 (lane 2) or HA−LYP−Q263 (lane 3). (B) Expression of LYP in transfected cells, detected by flow cytometry after gating on LYP-overexpressing cells. (C) pSLP-76 levels in TCR-stimulated cells transfected with LYP−R263 (continuous black graph) or with LYP−Q263 (dotted black graph) and gated as described, or in untransfected cells (tiled gray graph). pSLP-76 levels in unstimulated transfected cells were almost undetectable. The difference between LYP−R263 and LYP−Q263 calculated by Overton subtraction is shown above the graph. Data in panel (A–C) are representative of three experiments with similar results. (D) Activation of ERK2 is less inhibited in T-cells transfected with LYP−Q263. Myc-tagged ERK2 was co-transfected in JTAg cells together with HA−LYP−R263 (lanes 1,2) or with HA−LYP−Q263 (lanes 3,4). Cells were left unstimulated (lanes 1,3) or were stimulated with C305 for 2′ (lanes 2,4). (a) Shows an anti-pERK2 blot, (b) shows an anti-ERK2 blot of anti-myc immunoprecipitations, and (c) shows anti-LYP blot of total lysates. Numbers below each lane indicate densitometry results. The figure shows one of two independent experiments with similar results. (**E**) Activation of an NFAT/AP1 reporter in T-cells transfected with LYP−R263 or LYP−Q263. JTAg cells were co-transfected with a 3xNFAT/AP1 luciferase reporter and LYP−R263 or LYP−Q263. Cells were stimulated for 7 h with OKT3, lysed and luciferase activity measured on cell lysates. The average ± SD stimulation-induced increase in the ratio between firefly and *Renilla* luciferase activities of lysates of cells transfected with LYP−R263 (filled squares, continuous line) or LYP−Q263 (open squares, dotted line)—both measured in triplicate—was plotted versus LYP expression in the same lysates as assessed by anti-HA western blot. Lines are non-linear fitting of data to a third-order polynomial. The figure shows one of two independent experiments with similar results.

frequency differences across ethnicities but it remains to be determined whether larger variation occurs across different European populations, analogous to what has been reported for the R620W SNP (13). Lastly, when we compared the sequences of the catalytic domains from all available LYP homologs in the NCBI (National Center for Biotechnology Information) database we observed that, with the exception of humans, who contain an R at position 263, the amino acid at the homologous site in all of the other species is invariably a Q (Fig. 5), demonstrating that the ancestral enzyme encodes Q at position 263. Because it has been hypothesized that the *PTPN22* locus is under positive selective pressure

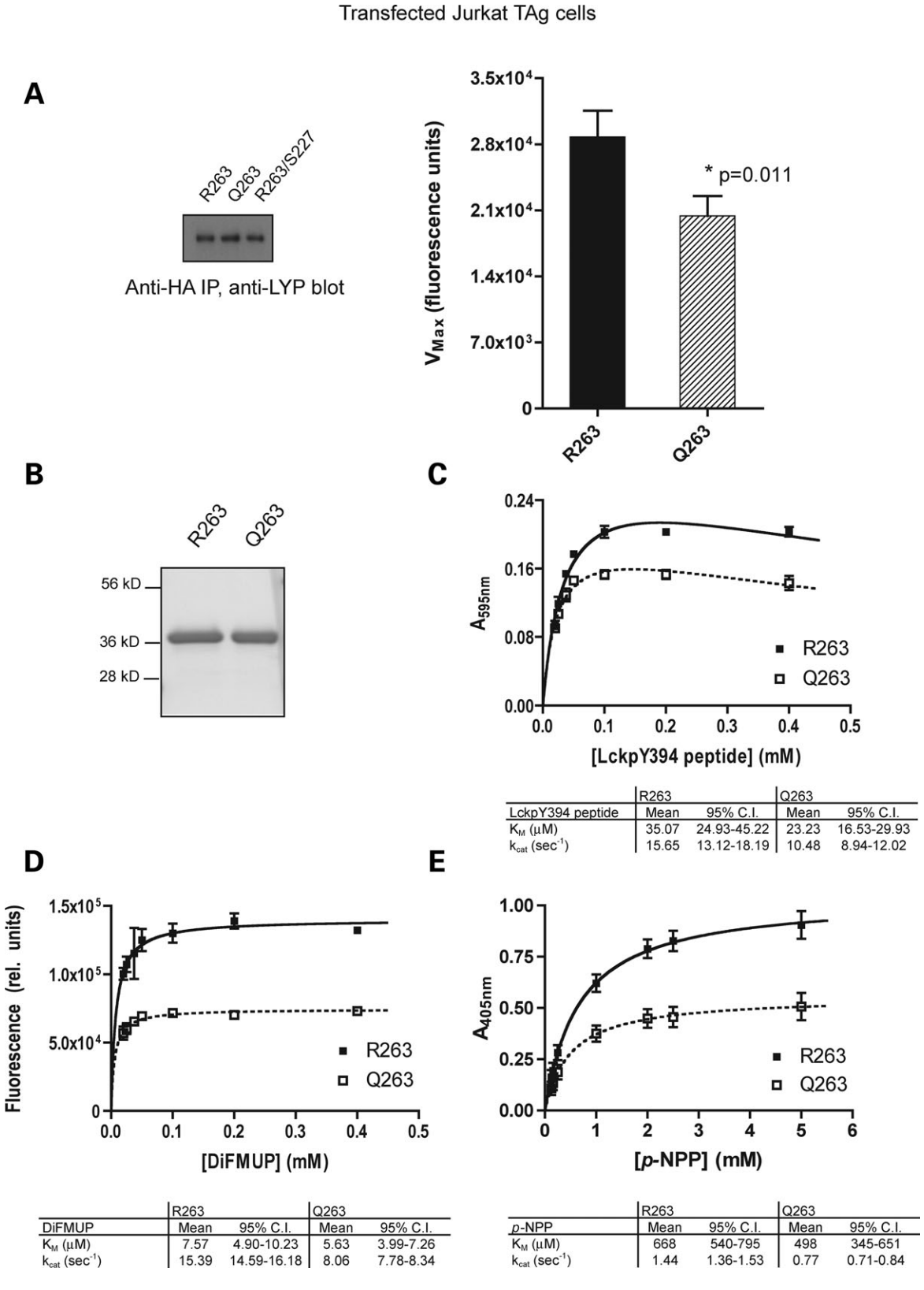

	R263		Q263	
LckpY394 peptide	Mean	95% C.I.	Mean	95% C.I.
K_M (μM)	35.07	24.93-45.22	23.23	16.53-29.93
k_{cat} (sec^{-1})	15.65	13.12-18.19	10.48	8.94-12.02

	R263		Q263	
DiFMUP	Mean	95% C.I.	Mean	95% C.I.
K_M (μM)	7.57	4.90-10.23	5.63	3.99-7.26
k_{cat} (sec^{-1})	15.39	14.59-16.18	8.06	7.78-8.34

	R263		Q263	
p-NPP	Mean	95% C.I.	Mean	95% C.I.
K_M (μM)	668	540-795	498	345-651
k_{cat} (sec^{-1})	1.44	1.36-1.53	0.77	0.71-0.84

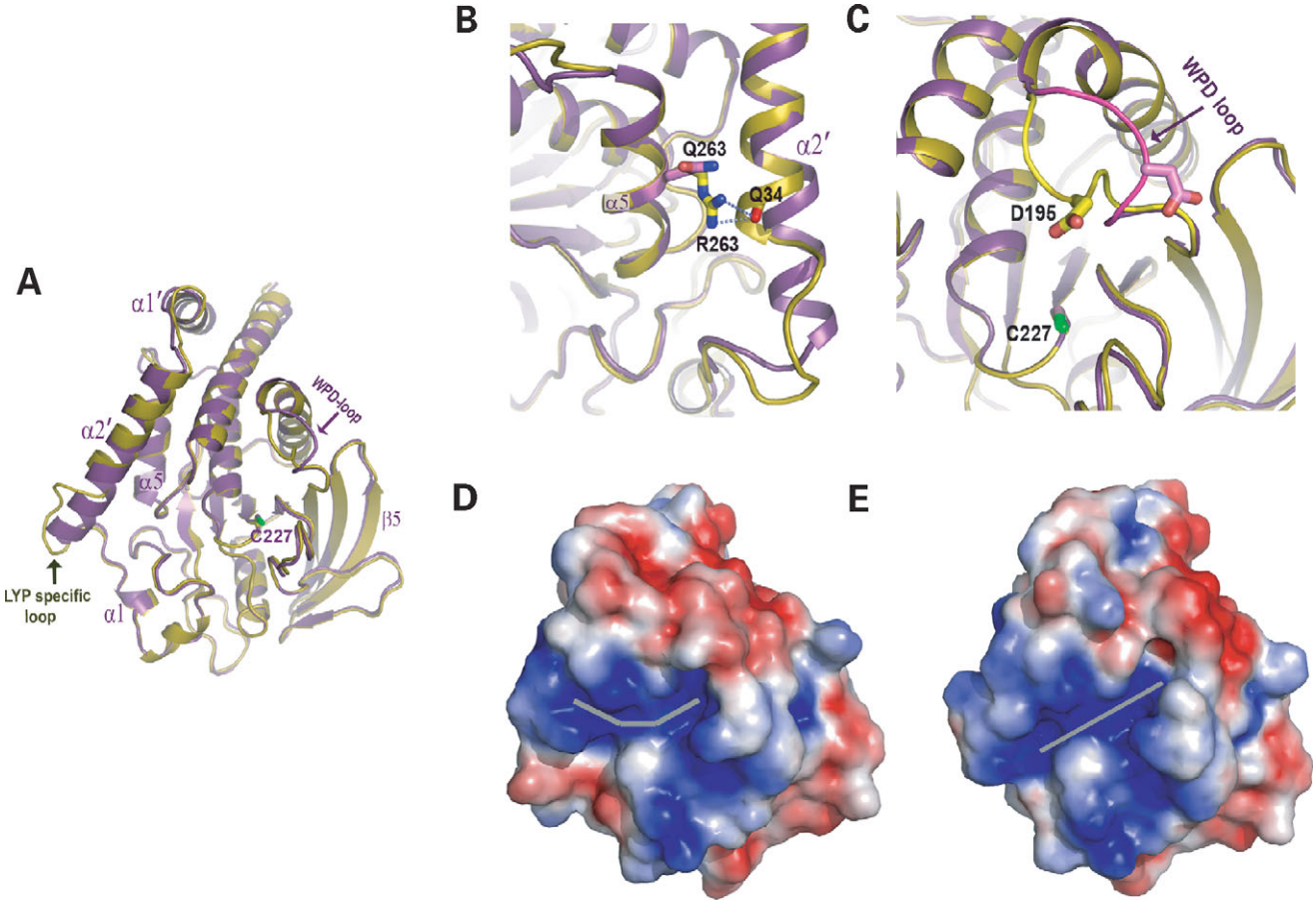

Figure 3. Structural basis for the reduced activity of LYP–Q263. (**A**) Superimposed structures of Cat-Q263 (purple) on Cat-R263 (yellow) show an open WPD loop and replacement of the LYP-specific loop with an extended helix in the mutant. The catalytic cysteine (C227) is shown in green. (**B**) The R263Q mutation in the LYP catalytic domain eliminates the contacts of R263 α5 helix to the α2′ helix on the main-chain carbonyl oxygen of Q34. (**C**) Movement of the WPD loop to the open conformation in R263Q. (**D,E**) Surface electrostatics of the (D) Cat-R263 and (E) Cat-Q263 structures. The deep electropositive cleft stretches from the active site to the LYP-specific loop, which is marked by gray sticks. When the LYP-specific region adopts the helical conformation in Cat-Q263 and shifts away from residue 263, the cleft conformation changes, which may reduce the efficiency of substrate processing by the enzyme.

(14), it would be interesting to determine whether the R263 allele also rose to such a high frequency in humans as a result of positive selection, since it can be considered a 'gain-of-function' allele relative to the ancestral Q263 variant.

DISCUSSION

Reduced TCR signaling has recently emerged as an important causal factor in the development of autoimmunity. In this regard, the R620W SNP in *PTPN22*, which reduces TCR signaling as a result of increased phosphatase activity, predisposes to several autoimmune disorders. In contrast, we demonstrate that a loss-of-function variant (R263Q), which is less effective in reducing TCR signaling, protects against SLE. The bi-directional association of *PTPN22* with autoimmunity has potentially important therapeutic implications since it has been proposed that inhibition of LYP activity, which would presumably enhance TCR signaling, could help

Figure 2. LYP–Q263 shows decreased phosphatase activity. (**A**) The Q263 allele shows lower phosphatase activity than R263. JTAg cells were transfected with HA–LYP–R263 or HA–LYP–Q263 or an inactive (C227S) variant of HA–LYP–R263. HA–LYP was immunoprecipitated from cell lysates and its phosphatase activity was assessed under V_{max} conditions using DiFMUP as a substrate. Left panel shows anti-HA blot of an aliquot of immunoprecipitations (IPs) from cells transfected with HA–LYP–R263 (lane 1), HA–LYP–Q263 (lane 2) or HA–LYP–C227S (lane 3). Histogram showing average ± SD activity of immunoprecipitated HA–LYP–R263 (black column) or HA–LYP–Q263 (shaded column), normalized for LYP expression as assessed by anti-HA blots of fractions of IPs taken before resuspension in the final phosphatase buffer, and corrected for the activity associated with HA–LYP–C227S immunoprecipitates. The statistical significance of the difference between LYP–Q263 and LYP–R263 was calculated by Student's *t*-test (*P*-value shown above the Q263 column). Figure shows one representative experiment of three independent replicates with similar results. (**B**) Coomassie-stained polyacrylamide gel showing 300 ng of Cat-R263 (lane 1) or Cat-Q263 (lane 2). (**C**–**E**) Activity of Cat-R263 (continuous graphs) and Cat-Q263 (dotted graphs) on three different substrates. Panels show activity on 14LckpY394, a 14 amino acid phospho-peptide ARLIEDNE(pY)TAREG, derived from the Tyr394 auto-phosphorylation site of Lck (C), or *p*-NPP (D), or DiFMUP (E). The average ± SD activity of Cat-R263 (filled squares) and Cat-Q263 (open squares) measured in triplicate was plotted versus substrate concentration, and data were fitted to the Michaelis–Menten equation (for *p*-NPP and DiFMUP) or the Michaelis–Menten with substrate inhibition (for the 14LckpY394 peptide) equations (continuous and dotted lines). Calculated catalytic parameters with 95% CI are reported below each graph.

Table 1. Data collection and refinement statistics for Cat structure

Crystal cell parameters	
Space group	P1
Cell dimensions	
(a, b, c in Å)	41.597, 57.934, 67.869
(α, β, γ in °)	90.069, 90.041, 105.689
Data collection statistics	
Resolution range (Å)	50.0–2.65
Observations	42 970
Unique reflections	16 878
Completeness (%)	95.1 (86.3)
R_{sym} (%) (last bin)	8.6 (26.0)
I/s (last bin)	16.1 (4.0)
Refinement statistics	
Resolution range (Å)	40.0–2.65
R_{cryst} (%)	21.6
R_{free} (%)	27.8
RMS deviation	
Bond length (Å)	0.009
Bond angle (°)	1.9
Average B factor (Å^2)	44.3

Note: $R_{sym} = \sum_{ij} |I_i(j) - <I(j)>| / \sum_{ij} I_i(j)$, where $I_i(j)$ is the i-th measurement of reflection j and $<I(j)>$ is the overall weighted mean of i measurements. $R_{cryst} = \Sigma hkl||Fo|-|Fc||/\Sigma hkl|Fo|$, 7% of the reflections were excluded for the R_{free} calculation.

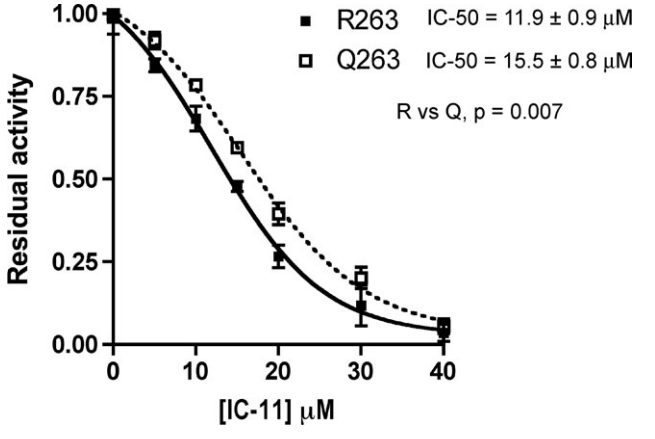

Figure 4. R263Q polymorphism affects inhibition of LYP by a small molecule inhibitor which interacts with the LYP-specific loop. Graph shows dose–response inhibition of Cat-R263 (filled squares and continuous line) or Cat-Q263 (open squares and dotted line) by IC-11, using the 14LckpY394 peptide as substrate. The reaction was carried out for 4 min using equal units of enzyme, and 30 μM substrate (this concentration is within the 95% CI of the K_M of both enzymes) in phosphatase buffer. The average ± SD activity of Cat-R263 (filled squares) and Cat-Q263 (open squares) measured in triplicate was plotted versus inhibitor concentration. The data were fitted to a Boltzmann sigmoidal, in order to calculate IC-50 (continuous and dotted lines). The statistical significance of the difference between Cat-Q263 and Cat-R263 was calculated by two-tailed paired Student's t-test (P-value shown above the graph). The figure shows one of two independent experiments with similar results.

prevent or treat such diseases (10). Stimulation of the TCR through a different mechanism has been shown to have curative effects in mouse models of T1D and to benefit human autoimmunity patients (15). In addition, the allele-specific inhibitory effect of IC-11 on LYP activity has implications for individualized therapeutic strategies (16). Our data suggest that patients carrying the Q263 variant might not benefit as much as non-carriers from inhibitors of LYP. Moreover, these experiments provide independent confirmation of our structural derivation as well as the interaction model proposed by Yu *et al*. for IC-11.

Considering that the PTPN22 R620W polymorphism predisposes to several autoimmune diseases, it is likely that the PTPN22 Q263 allele associates with multiple autoimmune diseases as well. For example, recently Skinningsrud *et al*. (17) reported a protective trend for the Q263 allele in Addison's disease. However, compared with the predisposition conferred by the R620W variant, the protective effect of R263Q appears to be weaker and, interestingly, it does not extend to T1D (12). One explanation for this observation is that a loss-of-function effect on TCR signaling is more easily compensated for than a gain-of-function effect. In addition, the quantitative thresholds between TCR signaling and the development of disease pathology are likely different in various autoimmune diseases. We speculate that for example a larger reduction in signal transduction through the TCR may be required for predisposition to SLE than to T1D. Experimental evidence is required to determine whether this model is indeed biologically plausible.

MATERIALS AND METHODS

Human subjects and genotyping

The Spanish, Argentinean and Italian SLE Cases and their clinical characteristics have all been previously described (18,19). The 457 European-derived SLE patients recruited in CA, USA, were an extension of the previously reported 60 multiplex and 258 simplex SLE families (20) and 358 normal Controls of European descent were also ascertained at the same site. In addition, 122 SLE patients and 209 Controls of European ancestry were recruited in Houston, TX, USA, as described (21). For the US cohort, self-reported ethnic origin of the four grandparents of the SLE patient and Controls (if known) were used to classify European ancestry. All cases fulfill the 1982 American College of Rheumatology criteria for the classification of SLE (22). All participating subjects provided informed consent for the study. The study was approved by the various Institutional Review Boards and Ethnical Committees at each of the participating locations. The genotyping for SNP rs33996649 was performed using a Custom-Taqman-SNP-Genotyping-Assay (Applied Biosystems, Foster City, CA, USA). The primer sequences were: forward 5′ TTTGAACTAATGAAGGCCTCTGTGT 3′ and reverse 5′ ATTCCTGAGAACTTCAGTGTTTTCAGT 3′. The specific minor groove binder probe sequences were 5′ TTGATCCGGGAAATG 3′ and 5′ TTGATCCAGGAAATG 3′.

Plasmids, antibodies and reagents

Full-length LYP was cloned in the *Bam*HI site of the plasmid pEF5 (23), which allows the expression of constructs in fusion with an N-terminal HA tag, and under control of the EF1alpha (elongation factor 1 alpha) promoter. Mutagenesis was performed by site-directed mutation primers, using *Pfu*-Ultra polymerase (Stratagene, San Diego, CA, USA) for PCR (polymerase chain reaction) amplification; all mutants were assessed by full-length sequencing. The anti-LYP antibody

Table 2. Frequency of *PTPN22* G788A (R263Q) genotypes in four cohorts of SLE patients and Controls and joint analysis with the Mantel–Haenszel test

Population		GG (R263/R263)	GA (R263/Q263)	AA (Q263/Q263)	Allele G (R263)	Allele A (Q263)	*P*-value (A allele)	OR (95% CI)
Spain	Cases (881)	846 (96.0)	35 (4.0)	0 (0)	1727 (98.0)	35 (2.0)	0.006	0.58 (0.38–0.86)
	Controls (1133)	1056 (93.2)	77(6.8)	0 (0)	2189 (96.6)	77 (3.4)		
Italy	Cases (357)	344 (96.4)	13 (3.6)	0 (0)	701 (98.2)	13 (1.8)	0.12	0.59 (0.30–1.18)
	Controls (371)	348 (93.8)	23 (6.2)	0 (0)	719 (96.9)	23 (3.1)		
Argentina	Cases (276)	268 (97.1)	8 (2.9)	0 (0)	544 (98.6)	8 (1.4)	0.37	0.69 (0.29–1.66)
	Controls (277)	265 (95.7)	12 (4.3)	0 (0)	542 (97.8)	12 (2.2)		
USA Caucasian	Cases (579)	564 (97.4)	15 (2.6)	0 (0)	1143 (98.7)	15 (1.3)	0.68	0.86 (0.40–1.84)
	Controls (567)	550 (97.0)	17 (3.0)	0 (0)	1117 (98.5)	17 (1.5)		
Pooled M–H	Cases (2093)	2022 (96.6)	71 (3.4)	0 (0)	4115 (98.3)	73 (1.7)	0.0017	0.63 (0.47–0.84)
	Controls (2348)	2219 (94.5)	129 (5.5)	0 (0)	4567 (97.2)	127 (2.8)		

Table 3. Frequency of *PTPN22* G788A (R263Q) genotypes in five ethnic groups

Population	*n*	GG R263/R263	GA R263/Q263	AA Q263/Q263	GA%
Caucasian	241	231	10	0	4.15
Hispanic	132	125	7	0	5.30
African-American	69	67	1	0	1.45
Asian	28	28	0	0	0.00

was purchased from R&D (Minneapolis, MN, USA). The monoclonal anti-HA antibody (clone 16B12) was purchased from Covance (Berkeley, CA, USA). The anti-ERK2 (C14) antibody and the monoclonal anti-Myc antibody (clone 9E10) were purchased from Santa Cruz Biotech (Santa Cruz, CA, USA). The PE(phycoerythrin)-conjugated anti-pSLP-76 (Tyr128) was purchased from BD Biosciences Pharmingen (San Jose, CA, USA). The anti-ACTIVE MAPK (anti-pERK) was from Promega (Madison, WI, USA).

Cell culture, transfections, cell stimulation

Jurkat T leukemia cells expressing SV-40 large T Antigen (JTAg) (24) were kept at logarithmic growth in Roswell Park Memorial Institute (RPMI) 1640 medium supplemented with 10% fetal calf serum, 2 mM L-glutamine, 1 mM sodium pyruvate, 10 mM HEPES pH 7.3, 2.5 mg/ml D-glucose, 100 units/ml of penicillin and 100 mg/ml streptomycin. Transfections were performed by electroporation as described (7). Short-term stimulation of JTAg cells was achieved by using C305 hybridoma (25) supernatants.

Phospho-flow cytometry

The anti-LYP antibody was conjugated with AF488 using a commercial conjugation kit (Pierce, Rockford, IL, USA) and the AF488-conjugated antibody was optimized for detection of LYP expression in flow cytometry (data not shown). Phospho-flow cytometry was performed on transfected JTAg cells following the manufacturer's instructions (BD Biosciences Pharmingen). Cells were fixed with BD Cytofix buffer, permeabilized using BD Phosflow buffer III and stained with AF488-conjugated anti-LYP and PE-conjugated anti-pSLP-76 (Tyr128) antibodies. Cell fluorescence was assessed on a Cytomics FC500 cytometer (Beckman Coulter, Fullerton, CA, USA) at the USC Immune Monitoring Core. Flow cytometry data analysis and graph preparation were carried out using FlowJo (Tree Star, Inc., Ashland, OR, USA). Differences between distributions were calculated by Overton subtraction (26). The sampling error in C305-stimulated JTAg cells was evaluated by measuring the average $\pm$ SD Overton subtraction% of three independent replicates and was $2.5 \pm 0.6\%$ for the anti-pSLP-76 antibody.

Immunoprecipitations and western blot analysis

For immunoprecipitations (IPs), cells were lysed in 20 mM Tris–HCl pH 7.4, 150 mM NaCl, and 1 mM EDTA (TNE buffer), with 1 mM phenylmethanesulphonylfluoride, 10 mg/ml

```
Homo sapiens       ---------------MDQREILQKFLDEAQSKKITKEEFANEFLKLKRQSTKYKADKTYP 45
Pan troglodites    ---------------MDQREILQKFLDEAQSKKITKEEFANEFLKLKRQSTKYKADKTYP 45
Macaca mulatta     ---------------MDQREILQKFLDEAQSKKINKEEFTNEFLKLKRQSTKYKADKTYP 45
Mus musculus       ---------------MDQREILQQLLKEAQKKKLNSEEFASEFLKLKRQSTKYKADKIYP 45
Rattus norvegicus  ---------------MDQREILQQLLKEAQKKKINREEFANEFLKLKRQSTKYKADKIYP 45
Bos taurus         LTGEMRGGRNHPGNLMDQREILQKFLDEAQHRKSNKEEFANEFLTLKRLSSKYKADKTYP 60
Gallus gallus      ---------------MDQREILLQNLERAQSRKLNQEAFADEFLKLKRQSTKYRSDKIYP 45
                                  ******* : *..** :* . * *:.***.*** *:**::** **

Homo sapiens       TTVAEKPKNIKKNRYKDILPYDYSR-VELSLITSDEDSSYINANFIKGVYGPKAYIATQG 104
Pan troglodites    TTVAEKPKNIKKNRYKDILPYDYSR-VELSLITSDEDSSYINANFIKGVYGPKAYIATQG 104
Macaca mulatta     TTVAEKPKNIKKNRYKDILPYDYSR-VELSLITSDEDSSYINANFIKGVYGPKTYIATQG 104
Mus musculus       TTVAQRPKNIKKNRYKDILPYDHSL-VELSLLTSDEDSSYINASFIKGVYGPKAYIATQG 104
Rattus norvegicus  TTVAQRPKNIKKNRYKDILPYDHSL-VELSLLTSDEDSSYINASFIKGVYGPRAYIATQG 104
Bos taurus         TTVAERPKNIKKNRYKDILPYDHSL-VELCMITSDEDSSYINANFIKGVYGPKTYIATQG 119
Gallus gallus      TVTAECPENIKRNRYKDILPYDHSR-VELSLITSDTDSHYINANFIKGVYGPRAYIATQG 104
                   *..*: *:***:**********:*  ***.::*** ** ****.********::******

Homo sapiens       PLSTTLLDFWRMIWEYSVLIIVMACMEYEMGKKKCE-RYWAEPGEMQLEFGPFSVSCEAE 163
Pan troglodites    PLSTTLLDFWRMIWEYSVLIIVMACMEYEMGKKKCE-RYWAEPGEMQLEFGPFSVSCEAE 163
Macaca mulatta     PLSTTLLDFWRMIWEYNVLIIVMACMEYEMGKKKCE-RYWAEPGEMQLEFGPFSISCEAE 163
Mus musculus       PLSTTLLDFWRMIWEYRILVIVMACMEFEMGKKKCE-RYWAEPGETQLQFGPFSISCEAE 163
Rattus norvegicus  PLSTTLLDFWRMIWEYRVLVIVMACMEFEMGKKKCE-RYWAEPGETQLQFGPFSISCETE 163
Bos taurus         PLPTTVLDFWRMIWEYSILIIVMACMEFEMGKKKCE-RYWAEPGDTQLQLGPFSISCEAE 178
Gallus gallus      PLPTTVTDFWRMIWEYEVLIVVMACMEFEMGKKKCE-RYWAEVGDSALQCGPFSITCEAE 163
                   **.**: ********* :*::******:******** ***** *:  *: ****::**:*

Homo sapiens       KRKSDYIIRTLKVKFNSETRTIYQFHYKNWPDHDVPSSIDPILELIW-DVRCYQEDDSVP 222
Pan troglodites    KRKSDYIIRTLKVKFNSETRTIYQFHYKNWPDHDVPSSIDPILELIW-DVRCYQEDDSVP 222
Macaca mulatta     KRKSDYIIRTLKVKFNSDTRTIYQFHYKNWPDHDVPSSIDPILELIW-DVRCYQEDDSVP 222
Mus musculus       KKKSDYKIRTLKAKFNNETRIIYQFHYKNWPDHDVPSSIDPILQLIW-DMRCYQEDDCVP 222
Rattus norvegicus  KKKSDYKIRTLKAKFNSETRIVYQFHYKNWPDHDVPSSIDPILQLIW-DMRCYQEDDCVP 222
Bos taurus         NRKSDYTIRTLKAKFNSETRTIYQFHYKNWPDHDVPSSIDPILELIW-DVRCYQDDNSVP 237
Gallus gallus      EKKNEYVIRTLKVSLNEAVRTIHQFHYQNWPDHDIPSSIDPILELIG-EVRCYQPDDSIP 222
                   ::*.:* *****..:*. .* ::****:******:********:**  ::**** *:.:*

Homo sapiens       ICIHCSAGCGRTGVICAIDYTWMLLKDGIIPENFSVFSLIREMRTQRPSLVQTQEQYE-L 281
Pan troglodites    ICIHCSAGCGRTGVICAIDYTWMLLKDGIIPENFSVFSLIQEMRTQRPSLVQTQEQYE-L 281
Macaca mulatta     ICIHCSAGCGRTGVICAIDYTWMLLKDGIIPENFSVFSLIQEMRTQRPSLVQTQEQYE-L 281
Mus musculus       ICIHCSAGCGRTGVICAVDYTWMLLKDGIIPKNFSVFNLIQEMRTQRPSLVQTQEQYE-L 281
Rattus norvegicus  LCIHCSAGCGRTGVICAVDYTWMLLKDGIIPKNFSVFNLIQEMRTQRPSLVQTQEQYE-L 281
Bos taurus         ICIHCSAGCGRTGVLCAIDYTWMLLKDGIIPENFSVFSLIQEMRTQRPSLVQTQQQYE-L 296
Gallus gallus      ICIHCSAGCGRTGVVCAIDYTWKLLKDGIVPVNFSIFSLIQEMRTQRPSIVQTKEQYK-L 281
                   :**************:**:**** ******:* ***:*.**:********:***::**: *

Homo sapiens       VYNAVLE 288
Pan troglodites    VYNAVLE 288
Macaca mulatta     VYNAVLE 288
Mus musculus       VYSAVLE 288
Rattus norvegicus  VYSAVLE 288
Bos taurus         VYNAVLE 294
Gallus gallus      VYNAVIE 288
                   **.**:*
```

Figure 5. Q263 allele defines the ancestral LYP variant. Alignment of catalytic domains of LYP from *Homo sapiens* (gi:48928054), *Pan troglotides* (gi:114558717), *Macaca mulatta* (gi:109014421), *Mus musculus* (gi:6679555), *Rattus Norvegicus* (gi:157824150), *Bos taurus* (gi:119889627) and *Gallus gallus* (gi:118102481). The residue in position 263 is highlighted in gray.

aprotinin/leupeptin, 10 mg/ml soybean trypsin inhibitor, and 10 mM sodium orthovanadate. Anti-HA antibody was added to the lysates, followed by sepharose-conjugated Protein G Sepharose (GE healthcare, Piscataway, NJ, USA) to precipitate the antibody–antigen complex. The beads were washed four to five times in lysis buffer, and resuspended in SDS sample buffer. Proteins were run on denaturing SDS–polyacrylamide gels (Invitrogen, Carlsbad, CA, USA), and transferred to nitrocellulose filters (Hybond ECL, GE Healthcare). Western blots were performed using appropriate dilutions of unconjugated primary antibodies, followed by HRP(horseradish peroxidase)-conjugated secondary antibodies (purchased from GE Healthcare). Filters were then subjected to a chemiluminescent detection protocol using ECL Plus (GE Healthcare) followed by autoradiography (using films from Kodak, Rochester, NY, USA).

Luciferase assays

Luciferase assays were performed as previously described (7). The NFAT/AP1 reporter plasmid (kindly provided by Dr Gerald Crabtree, Stanford University, Stanford, CA, USA) carries three tandem copies of the distal NFAT/AP1 composite element of the human *IL2* promoter (24) which are cloned upstream of the minimal *IL2* promoter (from −89 to +51) and the luciferase reporter gene. The NFAT/AP1 reporter plasmid and the Control pGL3 plasmid, driving constitutive expression of *Renilla* luciferase, were co-transfected in JTAg cells with variable amounts of the appropriate HA–LYP constructs. Cells were subjected to TCR stimulation with anti-CD3 [OKT3, purified from hybridoma supernatants (27)] for 7 h. Luciferase assays were then performed in triplicate on cell lysates using the dual luciferase kit from Promega according to the manufacturer's instructions, and luminescence measured on a Perkin Elmer 1420 Multilabel Counter Victor III V plate reader (Perkin-Elmer, Turku, Finland). The difference in the ratio between firefly and *Renilla* luciferase activity in stimulated versus unstimulated cells (TCR-induced increased activation of reporter) was then plotted against the expression of LYP assessed by densitometric scanning of anti-HA blots of total lysates.

Purification of recombinant proteins

The catalytic domain (amino acid 2–309) of LYP–R263 or LYP–Q263 (Cat-R263 and Cat-Q263) were cloned between the *Bam*HI and the *Xho*I sites of the pET28a vector (EMD Chemicals, Gibbstown, NJ, USA) and expressed in BL21 *Escherichia coli* cells in fusion with a thrombin-cleavable N-terminal 6xHis tag. Recombinant Cat was isolated from lysates of IPTG(isopropyl β-D-1-thiogalactopyranoside)-induced bacteria by two steps of affinity chromatography. Bacterial lysates were loaded on a Ni^{2+}-NTA column (Qiagen, Inc., Valencia, CA, USA) and the untagged protein was eluted by incubating the column with thrombin, followed by removal of thrombin through a second step on a benzamidin-sepharose column. As shown in Fig. 2B, the purified proteins were evident as single 37 kDa bands on denaturing SDS–polyacrylamide gels and their purity was at least 99% by Coomassie staining. Protein concentration was quantified by assessing absorbance of protein solutions at 280 nm, and confirmed by comparison with BSA standards on Coomassie-stained SDS–denaturing gels.

Phosphatase assays

In order to detect the phosphatase activity of full-length LYP immunoprecipitated from transfected JTAg cells, immunoprecipitates were washed three times in 100 mM Bis–Tris pH 6.0, and resuspended in phosphatase buffer (50–100 mM Bis–Tris, pH 6.0, 1–5 mM DTT). IPs were incubated with 0.5 mM 6,8-di-fluoro-4-methylumbelliferyl phosphate (DiFMUP), and dephosphorylation of DiFMUP was monitored continuously by measuring the increase in fluorescence (λ_{exc}= 355 nm and λ_{em}= 460 nm) at 60 s intervals for 30 min. The LYP-attributable activity of IPs measured in triplicate was calculated by subtracting the aspecific activity (also measured in triplicate) of identical IPs performed from lysates of cells transfected with inactive LYP–S227. The LYP-attributable activity was subsequently normalized for LYP expression as assessed by anti-HA blots of fractions of IPs taken before resuspension in the final phosphatase buffer. The activity of Cat was detected in the phosphatase buffer using *para*-nitrophenylphosphate (*p*-NPP), or DiFMUP, or a 14 amino acid pTyr peptide ARLIEDNE(pY)TAREG, derived from the Lck-Tyr394 phosphorylation site (14LckpY394). Dephosphorylation of DiFMUP was detected as described earlier. When the pTyr-peptide was used as substrate, the reaction was stopped by addition of BIOMOL GREEN™ (Biomol International, LP, Plymouth Meeting, PA, USA) and the phosphate released was detected by measuring the absorbance at 595 nm. When *p*-NPP was used as substrate, the reaction was stopped by addition of 1.0 M NaOH, and the activity was detected by monitoring the absorbance of *para*-nitrophenol at 405 nm. Fluorescence and absorbance were measured using the previously mentioned plate reader. The phosphatase activity measured in triplicate was corrected for the aspecific signal of identical reactions performed also in triplicate without addition of enzyme. Data were fit to the Michaelis–Menten equation or to the Michaelis–Menten with substrate inhibition equation (28), and kinetic parameters were calculated for each substrate. Amount of enzymes and time of incubation in all phosphatase assays were optimized in order to ensure initial rate conditions.

Protein crystallization and structure solution

Crystallization and data collection. Crystals of the Cat-Q263 variant were obtained using the vapor diffusion method at 18°C using a precipitant containing 2.0 M ammonium sulfate, 1% ethanol, 0.2 M sodium-potassium phosphate in 0.1 M MES, pH 6.2 in the buffer and pH 5.8 in the drop. Crystals appeared within 3–5 days and grew to full size in 1.5 weeks. Plate-shaped crystals were flash frozen after a quick soaking in a cryo solution containing 15% glycerol, 2.0 M ammonium sulfate, 0.2 M sodium–potassium phosphate in 0.1 M MES (pH 6.2) and diffraction data up to 2.65 Å were collected at in-house R-AXIS IV++ image plate. The data were processed using HKL2000, and data statistics are shown in Table 1.

Structure determination and refinement. The structure of the Cat-Q263 variant was solved by molecular replacement method (MOLREP) using the coordinates of wild-type Cat as the search model. The residue at mutation site and some of its neighbors were mutated to Ala in the search model. The N-terminal $\alpha1'$ and $\alpha2'$ helices and several other loops were deleted to avoid model bias. The model was refined using alternate cycles of refinement in crystallography & NMR system (CNS) and model building in 'O'. The mutated residue, truncated helices, loops and the side chains were gradually added to the model, guided by the electron density map, and the model was refined further using the standard slow-cool and positional refinement protocols of CNS package using the data between 40 and 2.65 Å. The model was finally checked in a composite omit electron density map. Progressive inclusion of water molecules, the bound phosphate ion, and MES coupled with a few cycles of refinement yielded an R_{cryst} of 21.6% ($R_{free} = 27.8\%$). Refinement statistics are given in Table 1.

Statistical analysis, graphs and experimental error calculations

Allelic and genotypic frequencies were calculated and compared by χ^2 tests using the Statcalc software (Epi Info 2002; Centers for Disease Control and Prevention, Atlanta, GA, USA) or the Stata software version 8 (Stata Corp., College Station, TX, USA). Significance was calculated by 2×2 contingency table and Fisher's exact test, to obtain *P*-values, OR and 95% CI. Statistical significance was considered when $P < 0.05$. The Breslow–Day test was used to test for homogeneity of the stratum specific ORs. This test did not indicate significant departure from homogeneity ($P = 0.78$), thus we computed the Mantel–Haenszel test for an overall association between R263Q variant and SLE, after controlling for population. The Haploview software was used to obtain LD pairwise values. As an overall test for association of R263Q SNP independent of R620W, we performed a conditional Case–Control test implemented in the UNPHASED software (http://portal.litbio.org/Registered/Webapp/glue/). Graphs, curve fitting, and kinetic parameter calculations were performed using the Graphpad Prism software package (Graphpad, San Diego, CA, USA). Sequence alignment was performed using ClustalW (29). All SD of differences and ratios were calculated according to the error propagation rules described by Taylor (30).

ACKNOWLEDGEMENTS

We wish to thank Giuseppe Novelli, Pragna Patel and James MacMurray for critical review of the manuscript.

Conflict of Interest statement. The authors declare no competing financial interest.

FUNDING

This work was supported by a grant 1-2005-342 from the Juvenile Diabetes Research Foundation (JDRF) and grants from the American Autoimmune Related Disease Association (AARDA) and the Arthritis National Research Foundation (ANRF) to N.B., grant SAF2006-00398 from the Spanish Ministerio de Educacion y Ciencia to J.M., Y.H. and Z.-Y.Z. are supported by grant NIH RO1 CA126937. E.F. and V.O. are supported by 'Master and Back' fellowships from the Sardinian Regional Government. S.M.S. is supported by the NIH Training Grant in Cellular, Biochemical, and Molecular biology at USC.

AUTHOR CONTRIBUTIONS

V.O., E.F., S.M.S., L.Z. performed experiments; S.J.T. and J.D. crystallized and solved the structure; B.R. and J. H. carried out all the genotyping; N.O.-C., S.D., F.C.A., H.W., M.G.D., M.A.G.-G., B.S., M.A., and their multicenter collaborators provided lupus samples; Y.H. and Z.-Y.Z. provided the IC-11 inhibitor, J.M. and H.A. supervised the genotyping effort and analyzed data; X.J.C. supervised the structural biology effort and analyzed data; N.B. conceived and supervised the whole project and analyzed all the data.

The Italian Collaborative Group participants are: Maria Giovanna Danieli (Clinica Medica, Dipartimento di Scienze Mediche e Chirurgiche, Università Politecnica delle Marche, Ancona); Mauro Galeazzi (Department of Clinical Medicine, Rheumatology Unit, Siena University, Siena); Maria Grazia Sabbadini (IRCCS San Raffaele Scientific Institute, Milan); Sergio Migliaresi (Rheumatology Unit, Second University of Naples, Naples); Gian Domenico Sebastiani (UOC di Reumatologia Azienda Ospedaliera San Camillo-Forlanini, Roma).

The Spanish Collaborative Group participants are: Jose L. Callejas (Servicio Medicina Interna, Hospital Clínico San Cecilio, Granada); Juan Jiménez-Alonso and Mario Sabio (Servicio de Medicina Interna, Hospital Virgen de las Nieves, Granada); Julio Sánchez-Román and Francisco J. Garcia-Hernandez (Servicio de Medicina Interna, Hospital Virgen del Rocio, Sevilla); Enrique de Ramón y Mayte Camps (Servicio Medicina Interna, Hospital Carlos Haya, Malaga); Miguel Angel López-Nevot (Servicio de Inmunología, Hospital Virgen de las Nieves, Granada); Maria F. González-Escribano (Servicio de Inmunología, Hospital Virgen de las Nieves, Sevilla); Carmen Gutierrez and Ana Suarez (Hospital Universitario Central de Asturias, Oviedo); Carles Tolosa (Servicio Medicina Interna, Hospital Parc Taulí, Sabadell); Luisa Micó (Servicio Medicina Interna, Hospital La Fe, Valencia).

REFERENCES

1. Cloutier, J.F. and Veillette, A. (1999) Cooperative inhibition of T-cell antigen receptor signaling by a complex between a kinase and a phosphatase. *J. Exp. Med.*, **189**, 111–121.
2. Wu, J., Katrekar, A., Honigberg, L.A., Smith, A.M., Conn, M.T., Tang, J., Jeffery, D., Mortara, K., Sampang, J., Williams, S.R. *et al.* (2006) Identification of substrates of human protein-tyrosine phosphatase PTPN22. *J. Biol. Chem.*, **281**, 11002–11010.
3. Bottini, N., Musumeci, L., Alonso, A., Rahmouni, S., Nika, K., Rostamkhani, M., MacMurray, J., Meloni, G.F., Lucarelli, P., Pellecchia, M. *et al.* (2004) A functional variant of lymphoid tyrosine phosphatase is associated with type I diabetes. *Nat. Genet.*, **36**, 337–338.

4. Begovich, A.B., Carlton, V.E., Honigberg, L.A., Schrodi, S.J., Chokkalingam, A.P., Alexander, H.C., Ardlie, K.G., Huang, Q., Smith, A.M., Spoerke, J.M. *et al.* (2004) A missense single-nucleotide polymorphism in a gene encoding a protein tyrosine phosphatase (PTPN22) is associated with rheumatoid arthritis. *Am. J. Hum. Genet.*, **75**, 330–337.
5. Kyogoku, C., Langefeld, C.D., Ortmann, W.A., Lee, A., Selby, S., Carlton, V.E., Chang, M., Ramos, P., Baechler, E.C., Batliwalla, F.M. *et al.* (2004) Genetic association of the R620W polymorphism of protein tyrosine phosphatase PTPN22 with human SLE. *Am. J. Hum. Genet.*, **75**, 504–507.
6. Lee, Y.H., Rho, Y.H., Choi, S.J., Ji, J.D., Song, G.G., Nath, S.K. and Harley, J.B. (2007) The PTPN22 C1858T functional polymorphism and autoimmune diseases – a meta-analysis. *Rheumatology (Oxford)*, **46**, 49–56.
7. Vang, T., Congia, M., Macis, M.D., Musumeci, L., Orru, V., Zavattari, P., Nika, K., Tautz, L., Tasken, K., Cucca, F. *et al.* (2005) Autoimmune-associated lymphoid tyrosine phosphatase is a gain-of-function variant. *Nat. Genet.*, **37**, 1317–1319.
8. Rieck, M., Arechiga, A., Onengut-Gumuscu, S., Greenbaum, C., Concannon, P. and Buckner, J.H. (2007) Genetic variation in PTPN22 corresponds to altered function of T and B lymphocytes. *J. Immunol.*, **179**, 4704–4710.
9. Siggs, O.M., Miosge, L.A., Yates, A.L., Kucharska, E.M., Sheahan, D., Brdicka, T., Weiss, A., Liston, A. and Goodnow, C.C. (2007) Opposing functions of the T cell receptor kinase ZAP-70 in immunity and tolerance differentially titrate in response to nucleotide substitutions. *Immunity*, **27**, 912–926.
10. Yu, X., Sun, J.P., He, Y., Guo, X., Liu, S., Zhou, B., Hudmon, A. and Zhang, Z.Y. (2007) Structure, inhibitor, and regulatory mechanism of Lyp, a lymphoid-specific tyrosine phosphatase implicated in autoimmune diseases. *Proc. Natl Acad. Sci. USA*, **104**, 19767–19772.
11. Carlton, V.E., Hu, X., Chokkalingam, A.P., Schrodi, S.J., Brandon, R., Alexander, H.C., Chang, M., Catanese, J.J., Leong, D.U., Ardlie, K.G. *et al.* (2005) PTPN22 genetic variation: evidence for multiple variants associated with rheumatoid arthritis. *Am. J. Hum. Genet.*, **77**, 567–581.
12. Zoledziewska, M., Perra, C., Orru, V., Moi, L., Frongia, P., Congia, M., Bottini, N. and Cucca, F. (2008) Further evidence of a primary, causal association of the PTPN22 620W variant with type 1 diabetes. *Diabetes*, **57**, 229–234.
13. Gregersen, P.K., Lee, H.S., Batliwalla, F. and Begovich, A.B. (2006) PTPN22: setting thresholds for autoimmunity. *Semin. Immunol.*, **18**, 214–223.
14. McPartland, J.M., Norris, R.W. and Kilpatrick, C.W. (2007) Tempo and mode in the endocannaboinoid system. *J. Mol. Evol.*, **65**, 267–276.
15. Chatenoud, L. (2006) CD3-specific antibodies as promising tools to aim at immune tolerance in the clinic. *Int. Rev. Immunol.*, **25**, 215–233.
16. Liggett, S.B., Cresci, S., Kelly, R.J., Syed, F.M., Matkovich, S.J., Hahn, H.S., Diwan, A., Martini, J.S., Sparks, L., Parekh, R.R. *et al.* (2008) A GRK5 polymorphism that inhibits beta-adrenergic receptor signaling is protective in heart failure. *Nat. Med.*, **14**, 510–517.
17. Skinningsrud, B., Husebye, E.S., Gervin, K., Lovas, K., Blomhoff, A., Wolff, A.B., Kemp, E.H., Egeland, T. and Undlien, D.E. (2008) Mutation screening of PTPN22: association of the 1858T-allele with Addison's disease. *Eur. J. Hum. Genet.*, **8**, 977–982.
18. Kozyrev, S.V., Lewen, S., Reddy, P.M., Pons-Estel, B., Witte, T., Junker, P., Laustrup, H., Gutierrez, C., Suarez, A., Francisca Gonzalez-Escribano, M. *et al.* (2007) Structural insertion/deletion variation in IRF5 is associated with a risk haplotype and defines the precise IRF5 isoforms expressed in systemic lupus erythematosus. *Arthritis Rheum.*, **56**, 1234–1241.
19. Kozyrev, S.V., Abelson, A.K., Wojcik, J., Zaghlool, A., Linga Reddy, M.V., Sanchez, E., Gunnarsson, I., Svenungsson, E., Sturfelt, G., Jonsen, A. *et al.* (2008) Functional variants in the B-cell gene BANK1 are associated with systemic lupus erythematosus. *Nat. Genet.*, **40**, 211–216.
20. Wu, H., Boackle, S.A., Hanvivadhanakul, P., Ulgiati, D., Grossman, J.M., Lee, Y., Shen, N., Abraham, L.J., Mercer, T.R., Park, E. *et al.* (2007) Association of a common complement receptor 2 haplotype with increased risk of systemic lupus erythematosus. *Proc. Natl Acad. Sci. USA*, **104**, 3961–3966.
21. Arnett, F.C., Thiagarajan, P., Ahn, C. and Reveille, J.D. (1999) Associations of anti-beta2-glycoprotein I autoantibodies with HLA class II alleles in three ethnic groups. *Arthritis Rheum.*, **42**, 268–274.
22. Hochberg, M.C. (1997) Updating the American College of Rheumatology revised criteria for the classification of systemic lupus erythematosus. *Arthritis Rheum.*, **40**, 1725.
23. Saito, K., Williams, S., Bulankina, A., Honing, S. and Mustelin, T. (2007) Association of protein-tyrosine phosphatase MEG2 via its Sec14p homology domain with vesicle-trafficking proteins. *J. Biol. Chem.*, **282**, 15170–15178.
24. Shaw, J.P., Utz, P.J., Durand, D.B., Toole, J.J., Emmel, E.A. and Crabtree, G.R. (1988) Identification of a putative regulator of early T cell activation genes. *Science*, **241**, 202–205.
25. Weiss, A. and Stobo, J.D. (1984) Requirement for the coexpression of T3 and the T cell antigen receptor on a malignant human T cell line. *J. Exp. Med.*, **160**, 1284–1299.
26. Overton, W.R. (1988) Modified histogram subtraction technique for analysis of flow cytometry data. *Cytometry*, **9**, 619–626.
27. Kung, P., Goldstein, G., Reinherz, E.L. and Schlossman, S.F. (1979) Monoclonal antibodies defining distinctive human T cell surface antigens. *Science*, **206**, 347–349.
28. Bardsley, W.G., Leff, P., Kavanagh, J. and Waight, R.D. (1980) Deviations from Michaelis–Menten kinetics. The possibility of complicated curves for simple kinetic schemes and the computer fitting of experimental data for acetylcholinesterase, acid phosphatase, adenosine deaminase, arylsulphatase, benzylamine oxidase, chymotrypsin, fumarase, galactose dehydrogenase, beta-galactosidase, lactate dehydrogenase, peroxidase and xanthine oxidase. *Biochem. J.*, **187**, 739–765.
29. Thompson, J.D., Higgins, D.G. and Gibson, T.J. (1994) CLUSTAL W: improving the sensitivity of progressive multiple sequence alignment through sequence weighting, position-specific gap penalties and weight matrix choice. *Nucleic Acids Res.*, **22**, 4673–4680.
30. Taylor, J.R. (1997) An introduction to error analysis. In *University Science Books*, 2nd edn.